ChemComm

COMMUNICATION

View Article Online
View Journal | View Issue

Cite this: *Chem. Commun.*, 2025, **61**, 7628

Received 14th January 2025,
Accepted 22nd April 2025

DOI: 10.1039/d5cc00209e

rsc.li/chemcomm

Dry liquid to Pickering-type emulsion: fabrication of non-spherical environmentally friendly microcapsules†

Benjamin T. Lobel, *[ab] Shota Sugiyama,[c] Oisín Owens,[a] Olivier J. Cayre *[a] and Syuji Fujii *[de]

Dry liquid was dispersed in oil to prepare water-in-oil Pickering-type emulsions. These emulsions were successfully converted into non-spherical biocompatible and degradable capsules *via* anionic polymerisation of butyl 2-cyanoacrylate at the water–oil interface. The non-spherical capsules were demonstrated to release rhodamine B in a controlled manner and to retain larger FITC-dextran molecules until acted upon by external ultrasound – making them ideal for prolonged encapsulation of large molecules such as enzymes.

Microcapsules are frequently employed in a variety of industries such as pharmaceutical, personal care and agrochemical.[1,2] Many of these microcapsules are formed from spherical emulsion templates. However, due to the low surface area to volume ratio of spheres and consequent low contact areas, adhesion to target substrates is often poor.[3] Furthermore, there is a growing need to develop microcapsules formulated from biocompatible/degradable materials. One potential solution to both these challenges is the preparation of environmentally friendly non-spherical microcapsules from emulsion templates. Non-spherical emulsion templates and the corresponding capsules can improve microcapsule applications by increasing the surface area-to-volume ratio, enhancing capsule-substrate contact, and reducing waste and material needs, whether this be in pesticides, therapeutics or cosmetics.[3–6] While some methods of anisotropic capsule formation exist within the literature utilising layer-by-layer assembly and nanolithography,[7] inorganic templates[8] or the use of external fields,[9] these methods are time-consuming, require specialised techniques and are difficult to scale. It is therefore desirable to develop simple, scalable, and environmentally friendly production methods of anisotropic capsule or emulsion templates.[10,11] One such method is the use of an emulsion template formed from dry liquids (DLs). DLs are bulk powders consisting of micro-sized particle-stabilised non-spherical liquid droplets (micro liquid marbles[12,13]) with reduced cohesion – that is, they flow freely.[14–17] These DLs have been reported as candidates for applications in gas storage *via* clathrate hydrate formation,[18] as a medium for heterogeneous catalysis[19] and in sensor-based technologies.[20,21] In addition, DLs have been shown to readily disperse in an oil phase to form Pickering-type emulsions that can then be used as a microcapsule template.[10,22] We report the formation of non-spherical capsules from a DL template loaded with poly(vinyl alcohol) (PVA) to increase droplet anisotropy, and rhodamine B and FITC-dextran (M_w 4.3 kDa) as simulant actives. The DLs were dispersed in oil and then used to produce degradable/biocompatible poly(butyl 2-cyanoacrylate) (PBCA) capsules *via* interfacial polymerisation (Fig. 1).[23–28] While alkyl cyanoacrylates have been previously used to form interfacial films and stabilise particle-adsorbed interfaces,[25–27] this is the first report of using a DL-based emulsion template for subsequent capsule formation. The DL template allows for long-term storage and control of dispersed phase loading without affecting capsule size, while increasing processing efficiency prior to dispersion in the oil phase. DL was prepared by adding PVA aqueous solution (25 wt%) to a powder bed of AEROSIL® RY 300 hydrophobised SiO_2 nanoparticles (NPs, 21–27 nm) and blended at high shear for 5 s (see ESI,† for detailed methods).[22,29]

Before the blending process, it was observed that the PVA solution did not effectively wet or absorb into the nanoparticle powder. This indicated that the SiO_2 nanoparticles had the capability to form DL.[22,29,30] The resultant DL was obtained as a free-flowing powder that could be easily handled (Fig. 1a). No bulk PVA solution was visible; the solution was completely

[a] *School of Chemical and Process Engineering, University of Leeds, Leeds, LS2 9JT, UK. E-mail: o.j.cayre@leeds.ac.uk*
[b] *School of Mathematics, Statistics, Chemistry and Physics, Murdoch University, Murdoch 6150, Australia. E-mail: b.t.lobel@murdoch.edu.au*
[c] *Division of Applied Chemistry, Environmental and Biomedical Engineering, Graduate School of Engineering, Osaka Institute of Technology, 5-16-1, Omiya, Asahi-ku, Osaka 535-8585, Japan*
[d] *Department of Applied Chemistry, Faculty of Engineering, Osaka Institute of Technology, 5-16-1 Omiya, Asahi-ku, Osaka 535-8585, Japan. E-mail: syuji.fujii@oit.ac.jp*
[e] *Nanomaterials Microdevices Research Center, Osaka Institute of Technology, 5-16-1, Omiya, Asahi-ku, Osaka 535-8585, Japan*

† Electronic supplementary information (ESI) available. See DOI: https://doi.org/10.1039/d5cc00209e

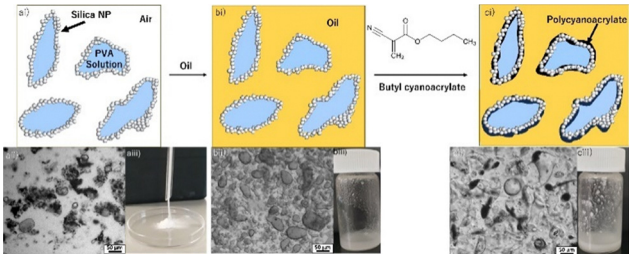

Fig. 1 (ai) Production of dry liquid (DL) *via* blending 25 wt% poly(vinyl alcohol) aqueous solution with hydrophobised SiO_2 nano particles. (bi) Dispersion of DL in oil phase to form Pickering-type water-in-oil emulsion. (ci) Addition of butyl 2-cyanoacrylate in oil solution to form a poly(butyl 2-cyanoacrylate) (PBCA) interfacial film *via* anionic polymerization, which results in formation of microcapsules. (aii)–(cii) Optical micrograph corresponding to respective steps. (aiii)–(ciii) Digital photographs corresponding to respective steps.

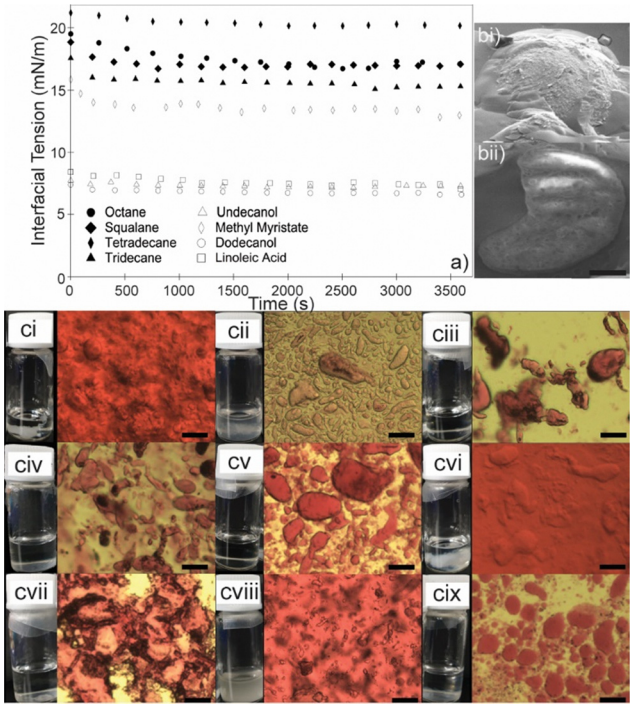

Fig. 2 (a) Interfacial tensions (IFTs) as measured by pendent drop tensiometry of 25 wt% poly(vinyl) alcohol (PVA) aqueous solution suspended in oil containing 2.5 wt% SiO_2-NPs. (bi) Cryo-SEM micrographs of Pickering emulsions produced from dispersing PVA based DL in squalane, (bii) emulsion after focused-ion beam, exposing internalised PVA, scale bar is 2.5 μm. (c) Pickering emulsions prepared by dispersing rhodamine B containing DL into oil phases: (ci) undecanol, (cii) methyl myristate, (ciii) squalane, (civ) tetradecane, (cv) tridecane, (cvi) dodecanol, (cvii) pentane, (cviii) linoleic acid, cix) octane (DL/oil, 20/80 wt%). Scale bars are 50 μm and photographs are PBCA formation 14 h after dissolving BCA in each oil.

encapsulated by the powder. This produced an easily scalable particle-stabilised water-in-air dispersion with a large surface area/volume ratio that could be transferred from the blending apparatus using a funnel without clogging (Video S1, ESI†). Optical micrographs revealed that the DL was comprised of anisotropic droplets covered by hydrophobic SiO_2-NPs, which formed irregularly shaped flocs (Fig. 1a). The DL was dispersed in oils with varying water solubility and interfacial tension (IFT) to assess emulsion stability (Fig. S2, ESI†), characterise the droplets, and enable subsequent interfacial polymerisation of butyl 2-cyanoacrylate (BCA). This resulted in Pickering-type water-in-oil emulsions (Fig. 2). The aqueous solution droplets were covered by the hydrophobic SiO_2-NPs as can be seen in Fig. 2bi, and were well dispersed in the oil media, as previously reported.[31] In all cases the droplets were observed to be non-spherical, which can be attributed to particles becoming jammed at the interface due to the crowding of the SiO_2-NPs and formation of a rigid particle network.[32,33] Specifically, the SiO_2-NPs become strongly adsorbed to the air–water interface as clustered aggregates and do not readily desorb.[34,35]

As a result, the droplets cannot relax to their thermodynamically favoured spherical shape from the initial anisotropic morphology obtained after the blending process, which is likely a result of interfacial crowding during mechanical elongation of the droplets formed by uneven shear. Indeed, as the droplets are deformed in shear, particles adsorb to the interface while simultaneously surface tension/Laplace pressure acts to restore droplet sphericity, which is opposed by the high viscosity of the PVA solution allowing for more particles to adsorb at the interface and become jammed.[35] Another possible route to interfacial jamming is arrested coalescence. Arrested coalescence may occur when partially coated droplets in the blender coalesce. As the interfacial area decreases, not all adsorbed particles can be redistributed, forming an interfacial network that prevents full coalescence leading to deformed droplets. In either proposed mechanism, this process was further enhanced by the high droplet viscosity due to the presence of the PVA.[35,36] To produce viable capsules a suitable oil is required. Specifically, an oil which may act as an emulsion continuous phase without resulting in unwanted polymerisation of the cyanoacrylate monomer, limiting polymerisation and film formation exclusively to the water/oil interface and thus forming discrete capsules. Additionally, the capsule core and rhodamine B should be insoluble in the oil to allow for processing and storage (Fig. S4, ESI†). Once the DL was dispersed in the oils, some leakage of the internalised rhodamine B could be observed in the more polar oils (alcohols, fatty acids) while pentane & octane resulted in evaporation of the oil phase and aggregation of the dispersed DL (Fig. 2). To investigate unwanted bulk polymerisation, BCA was dissolved in each of the oils to observe if any bulk polymerisation would occur, (Fig. 2 and Fig. S4, ESI†). In addition to these visual studies, pendent drop tensiometry was performed on each oil to quantify the interfacial activity of the SiO_2-NPs, and oil suitability (Fig. 2). Squalane was chosen as the most suitable oil due to significant decrease in IFT in the presence of the SiO_2 and the PVA (relative to a bare o/w interface), the lack of leakage/solubility of the aqueous phase into the bulk oil phase, the absence of unwanted bulk polymerisation observed during the aforementioned visual tests (Fig. 2 and Fig. S4, S5, ESI†) and biological/consumer significance.[37] In order to form capsules from the newly formed Pickering-type emulsions, BCA was dissolved in squalane and injected into the newly formed emulsions while under constant stirring. The BCA reacted exclusively at the water/oil interface producing a polymeric film. Flow cytometry was performed on

both DLs formed using water and 25 wt% PVA with a FlowCam device (Fig. 3). The use of flow cytometry allowed for the direct measurement of the 2D area of a particle and subsequent calculation of an equivalent spherical diameter. The measured D_n (the number average equivalent spherical diameter) for both the water and 25 wt% PVA samples was 12 μm and 16 μm, respectively, which is lower than reported in previous work.[22]

However, the D_v (calculated volume weighted average equivalent spherical diameter) measured in this work (38 and 35 μm respectively) is concordant with that previously reported when calculated using laser diffraction.[22] In addition to this, aspect ratio (AR) was also measured (Fig. 3). Capsules formed from DLs containing only water show a relatively low degree of anisotropy with 60% of capsules exhibiting an AR of >0.7, and over 20% with an AR of 1. Furthermore, the average of the AR distribution was calculated to be 0.75. This is in contrast with capsules formed using the 25 wt% PVA-DLs, whose average AR was calculated to be 0.59 where only 30% of the capsules had an AR >0.7, and less than 8% were observed to have an AR of 1. Moreover, only 63% of capsules were measured to have an AR greater than 0.5, indicating that the major axis of 37% capsules were more than twice in length when compared to their minor axis (Fig. 3 and Fig. S6, ESI†). These findings are concordant with the circle fit measurements that quantify the deviation from a projected circle on a 2D image of the particle (additional details in ESI†).[11] In the case of the water-only DL capsules, over 35% of the sample are perfectly spherical, and the distribution is heavily skewed towards sphericity (60% of capsules >0.85, average 0.83). This is in contrast with the PVA-DL capsule sample where less than 7% of the capsules are perfect spheres and only 20% of capsules >0.85 with an average circle fit of 0.62 – denoting a significant deviation from sphericity (Fig. 3).[11] Once formed, rhodamine B-containing capsules dispersed in squalane were placed in dialysis tubing and submerged in 40 wt% isopropanol (IPA) aqueous solution to evaluate capsule permeability (Fig. 4, further details in ESI†).

The capsules containing rhodamine B exhibited an initially slowed-release rate when compared to the DL templates (no PBCA shell), demonstrating a significant decrease in permeability, especially for the first 24 h (inset of Fig. 4), indicating that the PBCA outer layer was providing a barrier to release of the rhodamine B. However, after being subjected to the IPA solution for 80 h, both the capsule and DL samples had released 80% of their internalised rhodamine B, with nearly 100% released after 140 h. This was attributed to the small molecule rhodamine B (M_w 479 Da) being able to permeate through the porous polymeric structure at the interface resulting in eventual release. After the release studies, capsules were imaged using SEM for comparison with unmodified DL (Fig. 4b) The DL (Fig. 4bi) is an aggregate of particles with no obvious structure. This is in contrast with the PBCA capsules (Fig. 4bii) which have deflated on release and drying but retained their elliptical morphology indicating that they are not simply particles adsorbed at an interface but a polymeric film retaining its structure in the absence of any liquid. To further evaluate the release characteristics of the PBCA capsules, a larger (FITC-dextran, 4.3 kDa) molecule was investigated. No significant release was observed from the capsules after they were subjected directly to the 40 wt% IPA solution (no dialysis bag) for 24 h (Fig. 5b).

This is in contrast with the bare DL (no PBCA film) containing FITC-dextran (Fig. 5ai). The dextran is contained in the DL before being immersed in the IPA solution. However, after immersion in the IPA aqueous solution for 24 h (Fig. 5aii and iii) the fluorescent signal fully spreads to the continuous phase as the internal aqueous phase is completely miscible with the continuous phase and the dextran readily dissolves. This can be attributed to the complete solubilisation of the dispersed phase in the release medium, and consequently the lack of interface for particle adsorption. However, in the case of the PBCA capsules (Fig. 5bii) the fluorescent signal is still contained within the dispersed phase, and a polymeric barrier combined with the affixed particle shell mitigate direct interaction and subsequent leaching of the encapsulated core into the IPA

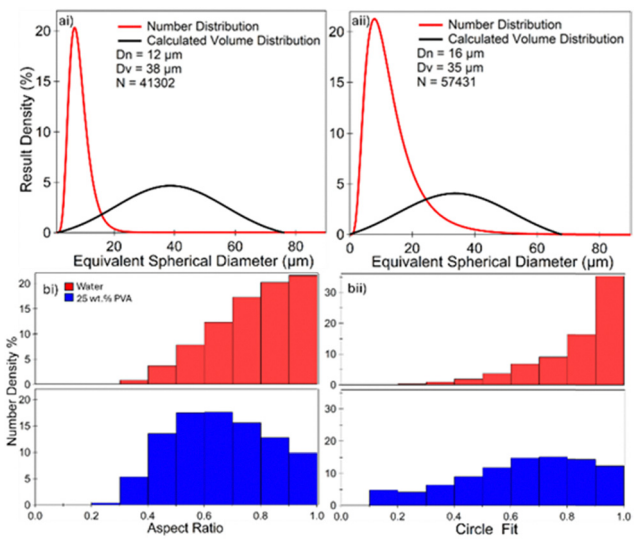

Fig. 3 (a) Size distribution of capsules dispersed in squalane as determined by flow cytometry. (i) DL formulated using 25 wt% PVA. (ii) DL formulated using water. (bi) AR of capsules formed from DL formulated using water and 25 wt% PVA. (bii) Circle fit of capsules formed from DL formulated using water and 25 wt% PVA. *N* is the number of particles analysed for all data presented in Fig. 3.

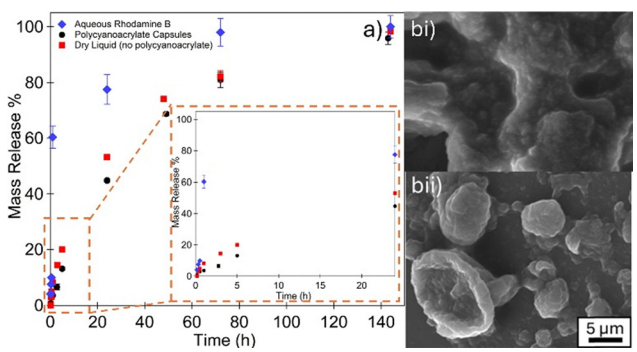

Fig. 4 (a) Release data of rhodamine B into 40 wt% IPA solution, from DL-based Pickering water-in-oil emulsion and PBCA capsules over 6 days. Inset: Release data for the first 24 h. (b) SEM micrographs, (i) DL after release, washing and drying. (ii) PBCA capsules after release, washing and drying.

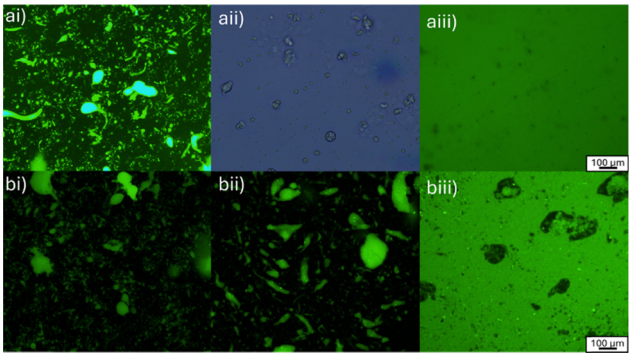

Fig. 5 (a) Micrographs of 25 wt% PVA-DL containing FITC-dextran. (i) Fluorescent image before immersion in 40 wt% aqueous solution of isopropanol (IPA). (ii) Bright field image after 24 h in 40 wt% IPA solution. (iii) Fluorescent image of (ii). (b) Fluorescent micrographs of PBCA capsules containing FITC-dextran prepared from the PVA-DL templates. (i) Before immersion in 40 wt% IPA solution. (ii) After 24 h immersion in 40 wt% IPA solution. (iii) PBCA capsules after 24 h immersion and ultrasonication in 40 wt% IPA solution.

solution. After probe sonication (Fig. 5biii), the capsules fracture, releasing fluorescent cargo into the continuous phase, with fractured capsules and debris appearing as dark patches within the micrograph. The FITC-dextran is too large to pass through the porous PBCA and SiO_2-NP network, so it remains trapped until the capsules rupture. While a smaller molecule such as rhodamine B was able to more readily permeate through the capsule shell, the fact that FITC-dextran can be contained within these capsules means they can be used for encapsulation of large molecules such as enzymes, for example in laundry products. For such application, the significant force applied during a washing cycle could result in rupture of the PBCA shells.[38]

We have demonstrated the fabrication of non-spherical capsules by dispersing DL into an oil phase, followed by anionic polymerisation of BCA at the oil–water interface. The capsules have an average D_n of 12 μm, D_v of 38 μm, AR and circle fit measurement of 0.59 and 0.62, respectively. Capsule concentration in dispersed media could be precisely controlled by tuning the added amount of DL into the oil phase prior to interfacial polymerisation. Once formed, these capsules demonstrated effective retention of FITC-dextran as a simulant large molecule or enzyme active until the capsules were ruptured *via* sonication and increased retention of rhodamine B when compared to an unmodified DL for the first 24 h of exposure to 40 wt% IPA. These capsules offer a scalable approach with desirable properties such as morphological anisotropy, degradability, and barrier function. Furthermore, once the DL is formed, the powder exhibits improved processing with respect to disperse phase loading and handling, appealing to both academia and industry.

This work was supported by a Grant-in-Aid for Scientific Research (B) (JSPS KAKENHI Grant No. JP20H02803 and JP24K01562) and Scientific Research on Innovative Areas "New Polymeric Materials Based on Element-Blocks (JSPS KAKENHI Grant No. JP15H00767)" as well as the EPSRC (EP/V027646/1). Mr Macauley Hough and Mr Stuart Micklethwaite (LEMAS) are thanked for Cryo/SEM imaging as well as Prof. Tomoyasu Hirai and Prof Yoshinobu Nakamura for their contribution. BTL thanks the RSC for a Researcher Development & Travel Grant (D23-3536371774).

Data availability

Data supporting this article have been included as part of the ESI.†

Conflicts of interest

There are no conflicts to declare.

Notes and references

1 R. Dubey, *et al.*, *Def. Sci. J.*, 2009, **59**, 82–95.
2 B. T. Lobel, *et al.*, *ACS Appl. Mater. Interfaces*, 2024, **16**, 40326–40355.
3 M. Cooley, *et al.*, *Nanoscale*, 2018, **10**, 15350–15364.
4 V. Kudryavtseva, *et al.*, *Adv. Mater.*, 2024, **36**, e2307675.
5 S. Roh, *et al.*, *Nat. Mater.*, 2019, **18**, 1315–1320.
6 P. Graf, *et al.*, *Langmuir*, 2006, **22**, 7117–7119.
7 V. Kudryavtseva, *et al.*, *Mater. Des.*, 2021, 202.
8 O. Shchepelina, *et al.*, *Macromol. Rapid Commun.*, 2010, **31**, 2041–2046.
9 R. B. Karyappa, *et al.*, *Langmuir*, 2014, **30**, 10270–10279.
10 A. M. Bago Rodriguez, *et al.*, *Curr. Opin. Colloid Interface Sci.*, 2019, **44**, 107–129.
11 B. T. Lobel, *et al.*, *Langmuir*, 2025, **41**, 550–562.
12 S. Fujii, *et al.*, *Adv. Funct. Mater.*, 2016, **26**, 7206–7223.
13 B. T. Lobel, *et al.*, *Adv. Powder Technol.*, 2021, **32**, 1823–1832.
14 B. P. Binks, *et al.*, *Nat. Mater.*, 2006, **5**, 865–869.
15 R. Murakami, *et al.*, *Adv. Funct. Mater.*, 2010, **20**, 732–737.
16 K. Shirato, *et al.*, *Soft Matter*, 2011, **7**, 7191–7193.
17 N. Manyuan, *et al.*, *J. Colloid Interface Sci.*, 2023, **649**, 581–590.
18 B. O. Carter, *et al.*, *Langmuir*, 2010, **26**, 3186–3193.
19 B. O. Carter, *et al.*, *Green Chem.*, 2010, **12**, 783–785.
20 N. Ono, *et al.*, *Adv. Sci.*, 2023, **10**, e2206097.
21 N. Shioda, *et al.*, *Mater. Horiz.*, 2023, **10**, 2237–2244.
22 K. Kido, *et al.*, *Adv. Powder Technol.*, 2017, **28**, 1977–1981.
23 E. Chiellini, *et al.*, *Prog. Polym. Sci.*, 2003, **28**, 963–1014.
24 A. T. Florence, *et al.*, *J. Pharm. Pharmacol.*, 1979, **31**, 422–424.
25 V. S. R. Jampani, *et al.*, *Adv. Mater.*, 2024, **36**, e2408243.
26 X. Lian, *et al.*, *Small*, 2023, **19**, e2301039.
27 J. M. Chin, *et al.*, *Chem. Commun.*, 2013, **49**, 493–495.
28 V. Bhagat, *et al.*, *Biomacromolecules*, 2017, **18**, 3009–3039.
29 M. Tenjimbayashi, *et al.*, *J. Mater. Chem. A*, 2024, **12**, 16343–16349.
30 M. Tenjimbayashi, *et al.*, *Adv. Mater.*, 2023, **35**, e2300486.
31 B. P. Binks, *et al.*, *Langmuir*, 2007, **23**, 9143–9146.
32 L. Shang, *et al.*, *Proc. Natl. Acad. Sci. U. S. A.*, 2024, **121**, e2403953121.
33 A. B. Subramaniam, *et al.*, *Nature*, 2005, **438**, 930.
34 M. Cui, *et al.*, *Science*, 2013, **342**, 460–463.
35 B. P. Binks and T. S. Horozov, *Colloidal Particles at Liquid Interfaces*, Cambridge University Press, 2006.
36 A. B. Pawar, *et al.*, *Soft Matter*, 2011, **7**, 7710–7716.
37 S. K. Kim, *et al.*, *Adv. Food Nutr. Res.*, 2012, **65**, 223–233.
38 P. H. Keen, *et al.*, *Langmuir*, 2014, **30**, 1939–1948.